Cell-Density Dependence of Host-Defense Peptide Activity and Selectivity in the Presence of Host Cells

Journal:	*ACS Chemical Biology*
Manuscript ID	cb-2016-00910t.R2
Manuscript Type:	Letter
Date Submitted by the Author:	n/a
Complete List of Authors:	Savini, Filippo; University of Rome Tor Vergata, Department of Chemical Sciences and Technologies Luca, Vincenzo; Sapienza Rome University, Department of Biochemical Sciences "A. Rossi Fanelli"; Istituto Pasteur-Fondazione Cenci Bolognetti Bocedi, Alessio; University of Rome Tor Vergata, Department of Chemical Sciences and Technologies Massoud, Renato; University of Rome Tor Vergata, Department of Experimental Medicine and Surgery Park, Yoonkyung; Chosun University, Department of Biotechnology Mangoni, Maria Luisa; Sapienza Rome University, Department of Biochemical Sciences "A. Rossi Fanelli"; Istituto Pasteur-Fondazione Cenci Bolognetti Stella, Lorenzo; University of Rome Tor Vergata, Department of Chemical Sciences and Technologies

Cell-Density Dependence of Host-Defense Peptide Activity and Selectivity in the Presence of Host Cells

Filippo Savini[1,a], Vincenzo Luca[2,a], Alessio Bocedi[1], Renato Massoud[3], Yoonkyung Park[4], Maria Luisa Mangoni[2], Lorenzo Stella[1,*].

[1]Department of Chemical Sciences and Technologies and [3]Department of Experimental Medicine and Surgery University of Rome Tor Vergata, 00133 Rome, Italy.

[2]Department of Biochemical Sciences "A. Rossi Fanelli", Istituto Pasteur Italia-Fondazione Cenci Bolognetti, Sapienza Rome University, 00185 Rome, Italy.

[4]Department of Biotechnology, Chosun University, 501–759 Gwangju, Korea.

[a] These authors contributed equally.

* To whom correspondence should be addressed:

Prof. Lorenzo Stella

Department of Chemical Sciences and Technologies

University of Rome Tor Vergata

Via della Ricerca Scientifica 1

00133, Rome, Italy

Tel.: +39-0672594463

E-mail: stella@stc.uniroma2.it

Abstract

Host-defense peptides (HDPs) are promising compounds against multidrug-resistant microbes. In vitro, their bactericidal and toxic concentrations are significantly different, but this might be due to the use of separate assays, with different cell-densities. For experiments with a single cell-type, the cell-density dependence of the active concentration of the DNS-PMAP23 HDP could be predicted based on the water/cell-membrane partition equilibrium, and exhibited a ~μM lower bound at low cell-counts. Based on these data, in the simultaneous presence of both bacteria and an excess of human cells one would expect no significant toxicity, but also inhibition of the bactericidal activity due to peptide sequestration by host cells. However, this inhibition did not take place in assays with mixed cell populations, showing that for the HDP esculentin1-a(1–21)NH_2 a range of bactericidal, non-toxic concentrations exists, and confirming the effective selectivity of HDPs. Mixed-cells assays might be necessary to effectively asses HDP selectivity.

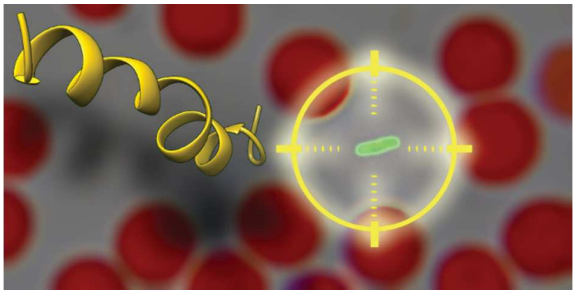

Host-defense peptides (HDPs) are produced by all living organisms as a first defense against pathogens. Multiple immunomodulatory functions of these peptides have been described in the last years (1), but one of their major activities is bactericidal, through the perturbation of the membrane permeability of microbial targets. This mechanism of action makes the development of bacterial resistance particularly unlikely (2,3), and for this reason these peptides are investigated as lead compounds to fight multidrug-resistant bacteria, a dramatic and increasing worldwide threat (4). However, several questions still limit their clinical applicability.

A major problem is related to HDP selectivity. *In vitro*, the majority of HDPs are toxic to mammalian cells only at concentrations higher than those needed for bactericidal activity (5). This behavior is presumably determined by the difference in lipid composition of membranes of the two cell-types, as studies on liposomes show a higher affinity for bilayers mimicking bacterial membranes (6). However, selectivity might be just an experimental artifact resulting from the very different conditions used in assays employed to determine antimicrobial and hemolytic activities, in particular the cell-density (5). Typically, minimal inhibitory concentrations (MICs) are determined with 5×10^5–1×10^6 colony-forming units (CFUs) per ml, while minimum hemolytic concentrations (MHCs) are measured in the presence of 5×10^8 cells/ml (5), and red blood cells (RBCs) have a membrane area approximately 10 times bigger than *E. coli* cells (7,8). In addition, the use of separate assays is based on the rather drastic assumption that the activity of HDPs against a given cell type is not influenced by the contemporary presence of different cells. However, in principle, when bacteria are in the presence of an excess of human cells, the peptide could be inactivated due to sequestration by host cells. Other important problems relate to the physiological function of HDPs, i.e. whether the relatively high peptide concentration needed to kill bacteria can be reached *in vivo* and whether their prevalent activity is bactericidal or immunomodulatory (9). Clarifying all these issues is essential, since they bear directly on how HDPs are currently screened and optimized.

A recently blooming approach to tackle these questions extends to real cells the quantitative physico-chemical experiments normally performed on model membranes (10–14). Recently, we measured the association to the membranes of *E. coli* cells of a fluorescently-labeled analogue of the cathelicidin HDP

PMAP-23 (15) (DNS-PMAP23, sequence in Scheme 1), and determined the threshold value of peptide molecules that must bind to the membranes of a single cell to kill it (11). Based on these results, in the present work we theoretically predicted an unexpected behavior of peptide activity as a function of the density of cells. We also optimized three assay protocols that allowed us to test experimentally this prediction by studying the bactericidal and hemolytic activities in a wide range of cell-density values, and to determine both activities under more realistic conditions, *i.e.* with both cell types present at the same time.

The so-called "inoculum effect" is a well-known dependence of the MIC of traditional antibiotics on the size of the bacterial inoculum in the growth medium, with the first studies dating back to the 1940s (16). By contrast, to the best of our knowledge, the cell-density dependence of HDP activity has not been investigated before. In a previous study (11), we showed that association of at least T_B=1.1x10^7 DNS-PMAP23 molecules to the membranes of each cell is needed to cause the death of 99.9% bacteria, *i.e.* the % reduction in viable cells normally used to define the minimum bactericidal concentration (MBC) (17). In addition, the measured peptide/cell-membranes association curves (see Supporting Information [SI], Supplementary Figure 1) exhibited a behavior that deviated only slightly from an ideal partition (11,18,19), where the fraction of membrane-associated peptide f_B dependence on bacterial cell-density ([Bacteria]) can be described according to the following equation, derived in SI:

$$f_B = \frac{[Bacteria]/K^B_{app.}}{1+[Bacteria]/K^B_{app.}} \quad (1$$

By fitting the partition curve measured for 10 μM peptide concentration (11) with Equation 1, we obtained a value of the apparent partition constant of $K^B_{app.}$=1.8x10^8 bacterial cells/ml (Supplementary Figure 1). These data allow a calculation of the fraction of membrane-bound peptide, and thus of the number of membrane-associated peptides per cell, at any value of peptide concentration and cell density. Based on these data, we now derived an equation (see SI) to predict the minimum total peptide concentration in the sample able to reach the T_B threshold, and thus able to kill 99.9% of the bacteria (*i.e.* the MBC)

$$MBC = \left(1 + [Bacteria]/K^{B}_{app.}\right) MBC_{min.} \quad (2$$

with

$$MBC_{min.} = K^{B}_{app.} \frac{10^3}{N_A} T_B \quad (3$$

Here N_A is Avogadro's constant, *MBC and* $MBC_{min.}$ are expressed in moles/l, $K^{B}_{app.}$ and the bacterial cell density ([Bacteria]) are reported in cells/ml and T_B is in molecules per cell.

The MBC values calculated for DNS-PMAP23, according to Equation 2 are reported as a continuous line in Figure 1b, on a logarithmic scale. This Equation predicts a linear decrease in the MBC with decreasing cell density. However, it also makes a rather surprising prediction, i.e. that even when the cell-density becomes extremely low, the MBC does not decrease below a limiting value, equal to $MBC_{min.}$ (3.3 μM, in our case). This behavior might seem counterintuitive, because when the cell-density decreases, the total amount of cell-bound peptide necessary to cause bacterial death diminishes proportionally, simply because less cells need to be killed. Naively, this consideration would lead to the conclusion that, in the limit of [Bacteria]→0, also MBC→0. However, in the low cell-density regime, most of the peptide will stay free in solution. When [Bacteria]<<$K^{B}_{app.}$, Eq. 1, like any hyperbolic equation (such as a Langmuir binding isotherm or a Michaelis-Menten enzyme kinetics), can be approximated by a linear behavior, and therefore f_B decreases proportionally to [Bacteria]. As a consequence, the total peptide concentration needed in the sample to kill the bacteria remains constant (Equation 3).

A similar theoretical prediction (*i.e*. a linear dependence of MBC, with a nonzero intercept) has been recently reported for the trend of peptide membrane-perturbing activity with the concentration of liposomes (20). Those calculations were based on a complex model considering several aspects of the peptide and lipid bilayer behavior at the molecular level. By contrast, the present treatment shows that the predicted trend simply arises from a close to ideal partition equilibrium, without the need of any assumptions on molecular level events. In addition, our previous data on the partition equilibrium and on the value of the threshold T_B (11) allowed us to perform quantitative predictions in cells.

The behavior predicted by Equation 2 was verified by experimental measurements of MBCs. Figure 1 a reports the killing curves measured in the presence of different cell-densities, under the conditions determined previously (11), where the number of live bacteria in a control sample remains constant during the time of the experiment. The interval of cell-densities studied was chosen to cover a realistic range, considering as an upper limit the number of bacteria in an abscess, which may reach up to 10^9 bacterial cells per ml of pus (21). The behavior predicted above was actually observed, with the MBC never decreasing below 3 μM (Figure 1b). The agreement between the experimental data and the predicted curve (which is not a fit) was acceptable even quantitatively.

The simple experiment reported here shows that it is possible to predict the MBC at all cell-densities, by determining the threshold of cell-bound peptides necessary to kill a bacterium, and the equilibrium of peptide association to bacterial cells. This possibility was first proposed by Melo *et al.* in relation to binding studies on model membranes (22), and it is now demonstrated with studies on real bacteria. In addition, our data show that micromolar total peptide concentrations are necessary to kill the bacteria, even when they are present at low cell counts. Attaining such concentration values in the body by systemic administration of HDPs as drugs might prove problematic. On the other hand, some HDPs can naturally reach concentrations that are even significantly higher, for instance in the granules of leukocytes, in the immediate vicinity of degranulating phagocytes, at the bottom of intestinal crypts (1), in the hemolymph of insects after a bacterial infection (23), or on the skin of some frogs (24). In addition, often multiple HDPs act at the same time and can exhibit synergism (25). However, for peptides whose physiological concentrations are lower than micromolar, other functions, such as immunomodulation, might be more important than direct bacterial killing (1).

The considerations that led to the prediction of a lower bound for the active concentration, irrespective of the target cell-density, are very general, and therefore a similar behavior could be conceived also for the toxic peptide activity against host cells. To test this hypothesis, we extended our study to erythrocytes, as a convenient model to investigate peptide toxicity. Unfortunately, the high absorbance of the heme group prevented us from determining peptide binding to RBCs with the same spectroscopic approach used for

bacteria (11). However, we developed a protocol to measure hemolysis in the presence of erythrocyte cell-densities varying in a range of 4 orders of magnitudes. We observed a cell-density dependence of peptide hemolytic activity similar to our findings for bacteria, with a limiting value at low cell counts (Figure 2). From these data, through a fitting with Equation 2, an order of magnitude estimate can be obtained for the partition constant and for the threshold of bound peptides relative to the lysis of erythrocytes: $K^{E}_{app.}$~10^7 RBCs/ml and T_E~10^7 molecules/RBC (the *E* super/subscript indicate that these values refer to erythrocytes, rather than to bacteria). Even if this determination of the parameters is rather indirect, the estimate for the order of magnitude of $K^{E}_{app.}$ can be considered reliable, as it corresponds to the cell density for which the minimum active concentration doubles with respect to the limiting value at low cell counts (Equation 2), and the data of Figure 2 definitely indicate that this happens between 4.5x10^6 and 4.5x10^7 cells/ml. In discussing these findings, in comparison with the corresponding values for bacteria, it should be considered that the membrane area of RBCs is about ten times of *E. coli* cells, but also that different criteria were used to determine the bactericidal and hemolytic concentrations (99.9% killing for MBC and 50% hemolysis for $HC_{50\%}$). In addition, DNS-PMAP23 is a particularly challenging system for testing HDP selectivity, since this property was reduced with respect to the parent peptide by the introduction of the fluorescent label (11, 26). From the standard activity assays commonly performed to determine peptide activity and selectivity (see SI) we obtained for DNS-PMAP23 a MIC of 16 μM and a concentration causing 50% hemolysis ($HC_{50\%}$) of 29 μM, with a therapeutic index (*i.e.* the ratio between the two values) of only 1.8. The $K_{app.}$ values obtained for the two cell types are compatible with this limited selectivity. However, selectivity under realistic conditions would depend on the cell-densities of both cell types. To place these data in context, it should be considered that the RBC density in whole blood is of the order of 5x10^9 cells/ml (27). Therefore, by comparing the data reported in Figures 1 and 2, and extrapolating to the RBC density in blood, it would appear that peptide concentration values might exist for which even the marginally selective DNS-PMAP23 could be active, without being toxic.

This conclusion, however, rests on the assumption that separate assays with one cell-type only allow the prediction of the behavior in a mixture of bacteria and host cells. However, the bactericidal activity of the

peptide might be inhibited due to sequestration by the predominant host cells. A quantitative discussion of this hypothesis, based on equilibrium equations similar to Equation 2 is reported in the SI. Indeed, the partition constants reported above lead to the prediction that, when the RBC density exceeds $K_{app.}^{E}$, significant inhibition of the bactericidal activity should be observed. To test for this possibility, we developed a novel assay to measure bacterial killing and RBC lysis in the presence of both cell types (Figure 3). The conditions used were of 4.5×10^7 *E. coli* cells/ml and 4.5×10^8 RBCs/ml. Considering also the different size of the two cell types, these values represent a large excess of eukaryotic versus bacterial cell membranes. Rather surprisingly, we observed that the antimicrobial activity was not affected by the presence of RBCs (Figure 3a). Peptide toxicity, too, was the same in the absence or in the presence of the bacteria.

The lack of alteration of the hemolytic activity in the presence of bacteria is compatible with an equilibrium partition treatment: due to the excess of RBCs, the fraction of peptide bound to bacteria is negligible (see SI). By contrast, the peptide capability to maintain its bactericidal activity also in the presence of a large excess of erythrocytes contrasts with the prediction based on partition equilibria between water and the two cell types, since a large fraction of peptide molecules should be sequestered by RBCs. Therefore, our finding indicates that an equilibrium treatment is inadequate in the presence of both host and bacterial cells, and that other effects (such as a faster peptide binding to bacteria than to RBCs) might be important. Of course, further experiments are needed to clarify this point.

It is reasonable to assume that if the bactericidal activity of a peptide with low selectivity like DNS-PMAP23 was unaffected by the presence of erythrocytes, a more selective HDP would also be insensitive to the simultaneous presence of both cell types. To test this hypothesis, and to verify if our findings can be generalized to other peptides, the killing and hemolysis curves were measured for separated and mixed cell populations also for esculentin1-a(1–21)NH_2 [Esc(1–21)]. This peptide (sequence in Scheme 1) is a derivative of esculentin-1a, a HDP isolated from the skin of the *Pelophylax lessonae/ridibundus* frog, which has been demonstrated to be highly selective, with a therapeutic index of 77 for *E. coli* (28, 29). Also in this case, only a minor inhibition of the antibacterial activity was caused by the presence of a large excess of RBCs (Figure 3b). In addition, in contrast to what has been observed for DNS-PMAP23, Esc(1–21) was highly

active against bacteria, without being significantly toxic in a large range of concentrations. These results provide support for a possible direct bactericidal function of HDPs under realistic conditions. They also bode well for the possible therapeutic application of HDPs, at least for topical treatments, while systemic administration might be faced with other hurdles (sequestration by serum components, proteolytic degradation, rapid clearance, etc.). However, it should be noted that several reports exist regarding the efficacy of HDPs *in vivo* (30) and their ability to concentrate at sites of infection (31).

In conclusion, our findings can be summarized as follows: i) In the presence of one cell type only, the cell-density dependence of the active peptide concentration is determined by the peptide/cell binding equilibrium and can be predicted, based on the determination of the apparent water/cell-membrane partition constant and of the threshold of membrane-bound peptides per cell needed to cause death; ii) at low cell-densities, the MBC does not decrease below a minimum limit, which in our case was in the micromolar range. This finding begs the question whether these relatively high concentrations can be reached *in vivo*; iii) since both the peptide activity and toxicity depend on cell-density, the effective selectivity of HDPs depends on the amounts of host and target cells present; iv) at the same time, the antibacterial activity was not affected by the contemporary presence of a large excess of host cells, as could have been expected based on water/cell-membrane partition equilibria. This finding indicates that a reconsiderations of the protocols and assays currently used in the evaluation of HDP selectivity might be necessary. Extension of the present results to other peptides and cell types is essential, but due to the similarity of the properties of many HDPs, our conclusions might apply also to other systems.

NOTE ADDED IN PROOF

While the present work was under revision, an article by Wimley and coworkers was published online (32), reporting the inhibition of the bactericidal activity of some HDPs by an excess of RBCs. However, this effect was observed only when the peptide was preincubated with RBCs before adding the peptide/erythrocyte solution to bacteria. In agreement with our findings, no significant inhibition took place when the peptide

was added directly to a bacteria/RBCs mixture. The fact that bacterial killing depends on the order of addition of the various components in the assay strongly supports the hypothesis that kinetic effects might be important when different cell populations are present at the same time.

ASSOCIATED CONTENT

Supporting Information Available

Model for the interaction of HDPs with different cell populations and for the prediction of peptide activity, with derivation of Equations 1 and 2. Methods. This material is available free of charge *via* the Internet.

ACKNOWLEDGEMENTS

We thank G. Bocchinfuso and M. Venanzi for helpful discussions and the Korea NRF (2016R1A2A1A05005440 and NRF-2014K1A1A2064460), MIUR (PRIN 20157WW5EH) and University of Rome Tor Vergata (Consolidate the Foundations AMPSA) for financial support.

FIGURES

Scheme 1 Sequences of the peptides investigated.

DNS-PMAP23

Dansyl-RIIDLLWRVRRPQKPKFVTVWVR-NH_2

Esc(1-21)

GIFSKLAGKKIKNLLISGLKG-NH_2

Color code: acid, basic and hydrophobic residues;
Dansyl (DNS) = 5-(dimethylamino)naphthalene-1-sulfonyl.

Figure 1 Cell-density dependence of DNS-PMAP23 bactericidal activity.

a): Bactericidal activity in the presence of different *E. coli* cell densities.

b) Predicted (Equation 2) and experimental cell-density dependence of the MBC (defined as the concentration that causes the death of 99.9% of bacteria).

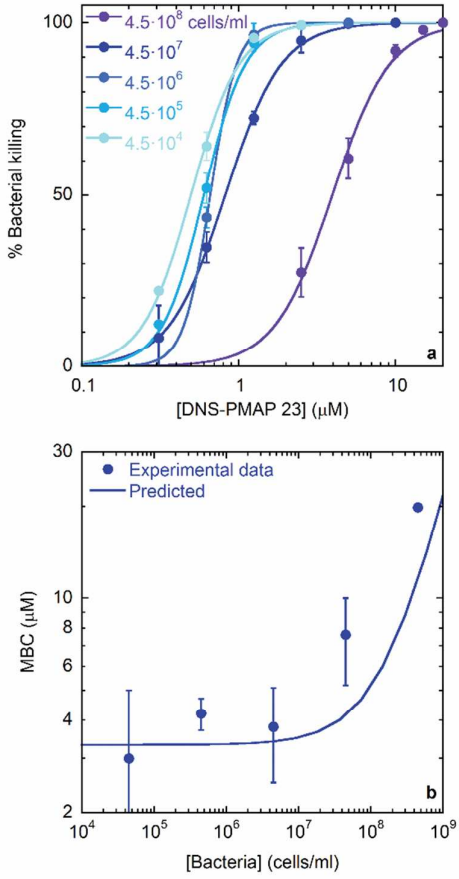

Figure 2 Cell-density dependence of DNS-PMAP23 hemolytic activity

a) curves of hemolytic activity determined in the presence of different RBC densities.

b) cell-density dependence of the peptide concentration needed to cause 50% hemolysis ($HC_{50\%}$). The continuous line is a fit with Equation 2.

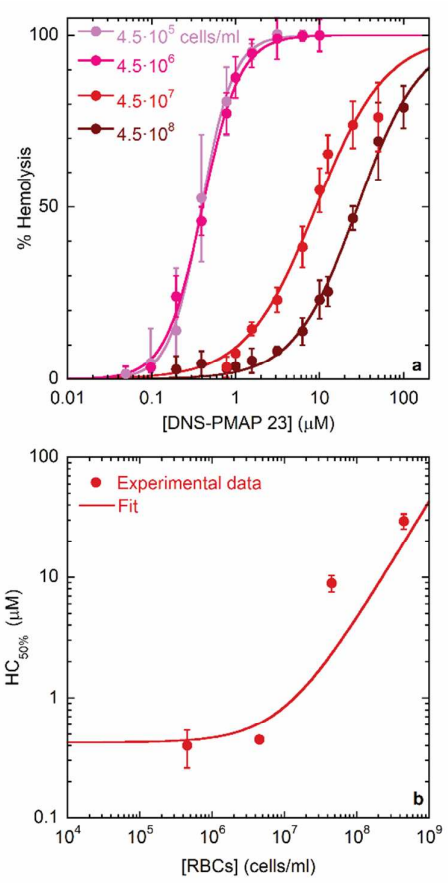

Figure 3 Bactericidal and hemolytic activities of DNS-PMAP23 (a) and Esc(1–21) (b) in the presence of both bacteria and erythrocytes or of one cell type only.

$4.5x10^7$ *E. coli* cells/ml, $4.5x10^8$ RBCs/ml.

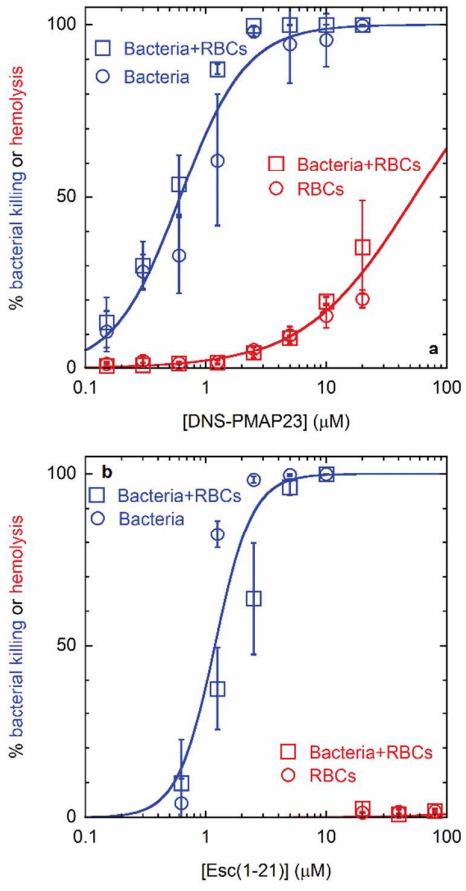

References

1. Hancock, R.E., Haney, E.F., Gill, E.E. (2016) The immunology of host defence peptides: beyond antimicrobial activity, *Nat Rev Immunol. 16*, 321–334.

2. Wimley, W.C. (2010) Describing the mechanism of antimicrobial peptide action with the interfacial activity model, *ACS Chem. Biol. 5*, 905–917.

3. Fox, J.C. (2013) Antimicrobial peptides stage a comeback, *Nat. Biotechnol*. *31*, 379−382.

4. Ventola, C.L. (2015) The antibiotic resistance crisis: part 1: causes and threats, *Pharm. Ther. 40*, 277–283.

5. Matsuzaki, K. (2009) Control of cell selectivity of antimicrobial peptides, *Biochim. Biophys. Acta 1788*, 1687–1692.

6. Bobone, S., Bocchinfuso, G., Park, Y., Palleschi, A., Hahm, K.S. and Stella L. (2013) The importance of being kinked: role of Pro residues in the selectivity of the helical antimicrobial peptide P5, *J Pept Sci. 19*, 758–769.

7. Yawata, Y. (2003) Cell membrane: the red blood cell as a model, WILEY-VCH, Weinheim.

8. Schulz, H. N., Jorgensen, B.B. (2001) Big bacteria*, Annu. Rev. Microbiol. 55*, 105−137.

9. Hilchie, A. L., Wuerth, K., and Hancock, R.E.W. (2013) Immune modulation by multifaceted cationic host defense (antimicrobial) peptides, *Nature Chem Biol*. *9*, 761–768.

10. Melo, N. M., Ferre, R., and Castanho, M.A.R.B. (2009) Antimicrobial peptides: linking partition, activity and high membrane bound concentrations, *Nat. Rev. Microbiol. 7*, 245−250.

11. Roversi, D., Luca, V., Aureli, S., Park, Y., Mangoni, M.L. and Stella, L. (2014) How many antimicrobial peptide molecules kill a bacterium? The case of PMAP-23, *ACS Chem Biol. 9*, 2003–2007.

12. Freire, J.M., Gaspar, D., Veiga, A.S. and Castanho, M.A. (2015) Shifting gear in antimicrobial and anticancer peptides biophysical studies: from vesicles to cells, *J Pept Sci. 21*, 178–185.

13. Malgieri, G., Avitabile, C., Palmieri, M., D'Andrea, L.D., Isernia, C., Romanelli, A. and Fattorusso, R. (2015) Structural basis of a temporin 1b analogue antimicrobial activity against Gram negative bacteria determined by CD and NMR Techniques in cellular environment, *ACS Chem. Biol.* 10, 965−969.

14. Choi, H., Rangarajan, N. Weisshaar, J.C. (2016) Lights, camera, action! antimicrobial peptide mechanisms imaged in space and time, *Trends Microbiol. 24*, 111–122.

15. Orioni, B., Bocchinfuso, G., Kim, J. Y., Palleschi, A., Grande, G., Bobone, S., Park, Y., Kim, J., Hahm, K.S., and Stella, L. (2009) Membrane perturbation by the antimicrobial peptide PMAP-23: A fluorescence and molecular dynamics study, *Biochim. Biophys. Acta 1788*, 1523−1533.

16. Brook, I. (1989) Inoculum effect, *Rev Infect Dis. 11*, 361–368.

17. Schwalbe, R., Steele-Moore, L. and Goodwin, A. C. (2007). Antimicrobial Susceptibility Testing Protocols, CRC Press, Boca Raton.

18. Stella, L., Mazzuca, C., Venanzi, M., Palleschi, A., Didonè, M., Formaggio, F., Toniolo, C., and Pispisa, B. (2004) Aggregation and water-membrane partition as major determinants of the activity of the antibiotic peptide trichogin GA IV, *Biophys. J. 86*, 936–945.

19. White, S. H., Wimley, W. C., Ladokhin, A. J., and Hristova, K., (1998) Protein folding in membranes: determining energetics of peptide-bilayer interactions, *Methods Enzymol.* 295: 62–87

20. Bagheri, A., Taheri-Araghi, S. and Ha, B.Y., (2015) How cell concentrations are implicated in cell selectivity of antimicrobial peptides, *Langmuir 31*, 8052–8062.

21. König, C., Simmen, H.P., and Blaser, J. (1998) Bacterial concentrations in pus and infected peritoneal fluid–implications for bactericidal activity of antibiotics, *J. Antimicrob. Chemother. 42*, 227−232.

22. Melo, N. M., Ferre, R., Feliu, L., Bardaji, E., Planas, M., and Castanho, M.A.R.B. (2011) Prediction of antibacterial activity from physicochemical properties of antimicrobial peptides, *PLoS One 6*, e28549.

23. Lemaitre, B. and Hoffmann, J. (2007) The Host Defense of Drosophila melanogaster, *Annu. Rev. Immunol. 25*, 697–743.

24. Mangoni, M. L., Di Grazia, A., Cappiello, F., Casciaro B. and Luca, V. (2016) Naturally occurring peptides from rana temporaria: antimicrobial properties and more, *Curr. Top. Med. Chem. 16*, 54–64.

25. Mangoni, M. L., and Shai, Y. (2009) Temporins and their synergism against Gram-negative bacteria and in lipopolysaccharide detoxification, *Biochim. Biophys. Acta 1788*, 1610–1619.

26. Kim, J.Y., Park, S.C., Yoon, M.Y., Hahm, K.S. and Park, Y. (2011) C-terminal amidation of PMAP-23: translocation to the inner membrane of Gram-negative bacteria, *Amino Acids 40*, 183–195.

27. Sender, R., Fuchs, S. and Milo, R. (2016) Are we really vastly outnumbered? Revisiting the ratio of bacterial to host cells in humans, *Cell 164*, 337–340.

28. Islas-Rodrìguez, A. E., Marcellini, L., Orioni, B., Barra, D., Stella, L. and Mangoni, M. L. (2009). Esculentin 1–21: a linear antimicrobial peptide from frog skin with inhibitory effect on bovine mastitis-causing bacteria, *J. Pept. Sci. 15*: 607–614.

29. Luca, V., Stringaro, A., Colone, M., Pini, A. and Mangoni, M.L. (2013) Esculentin(1–21), an amphibian skin membrane-active peptide with potent activity on both planktonic and biofilm cells of the bacterial pathogen Pseudomonas aeruginosa, *Cell Mol Life Sci. 70*, 2773–2786.

30. Zhang, L. and Falla, T.J. (2006) Antimicrobial peptides: therapeutic potential, *Expert Opin. Pharmacother. 7*, 653–663.

31. Bunschoten, A., Welling, M.M., Termaat, M.F., Sathekge, M. and Van leeuwen, F.W. (2013) Development and prospects of dedicated tracers for the molecular imaging of bacterial infections, *Bioconjug Chem. 24*, 1971–1989.

32. Starr, C.G., He, J. and Wimley, W.C. (2016) Host cell interactions are a significant barrier to the clinical utility of peptide antibiotics, *ACS Chem. Biol.* Doi: 10.1021/acschembio.6b000843.

33. Mangoni, M.L., Carotenuto, A., Auriemma, L., Saviello, M.R., Campiglia, P., Gomez-Monterrey, I., Malfi, S., Marcellini, L., Barra, D., Novellino, E. and Grieco, P. (2011) Structure-activity relationship, conformational and biological studies of temporin L analogues, *J Med Chem. 54*, 1298–1307.

SUPPORTING INFORMATION FOR

Cell-Density Dependence of Host-Defense Peptide Activity and Selectivity in the Presence of Host Cells

Filippo Savini[1,a], Vincenzo Luca[2,a], Alessio Bocedi[1], Renato Massoud[3], Yoonkyung Park[4], Maria Luisa Mangoni[2], Lorenzo Stella[1,*].

[1]Department of Chemical Sciences and Technologies and [3]Department of Experimental Medicine and Surgery University of Rome Tor Vergata, 00133 Rome, Italy.

[2]Department of Biochemical Sciences "A. Rossi Fanelli", Istituto Pasteur Italia-Fondazione Cenci Bolognetti, Sapienza University of Rome, 00185 Rome, Italy.

[4]Department of Biotechnology, Chosun University, 501–759 Gwangju, Korea.

[a] These authors contributed equally.

* To whom correspondence should be addressed:

Prof. Lorenzo Stella

Department of Chemical Sciences and Technologies

University of Rome Tor Vergata

Via della Ricerca Scientifica 1

00133, Rome, Italy

Tel.: +39-0672594463

E-mail: stella@stc.uniroma2.it

A SIMPLE MODEL PREDICTING PEPTIDE ACTIVITY AND SELECTIVITY BASED ON PEPTIDE-CELL ASSOCIATION DATA

This section describes a very simple model to predict peptide activity and selectivity. It is based on the idea that peptide activity is determined by how much peptide associates to the cell membranes, and by the amount of bound peptide needed to cause cell death/lysis of a single cell. In this view, selectivity is determined by the differences in these two factors for different cells and by cell concentrations.

Peptide partition between the aqueous phase and the cell membranes.

The association of a peptide to cell membranes can be treated as a partition between two immiscible phases (18, 19; reference numbers refer to the main text), defined by the following partition constant (assuming an ideal solution behavior):

$$K = \frac{x_m}{x_a} = \frac{\frac{n_m}{n_m+n_l}}{\frac{n_a}{n_a+n_w}} \quad \text{S1}$$

where x_m and x_a represent the molar fractions of the peptide in the membrane and aqueous phase, respectively. Similarly, n_m and n_a are the number of moles of peptide in the two phases, while n_l and n_w are the number of moles of membrane lipids and of water in the sample. Generally, it can be assumed that $n_w \gg n_a$ and $n_l \gg n_m$. Under this approximation,

$$K \cong \frac{\frac{n_m}{n_l}}{\frac{n_a}{n_w}} = \frac{n_m}{n_a} \cdot \frac{n_w}{n_l} \quad \text{S2}$$

By dividing both n_w and n_l by the total sample volume, the total molar concentrations of water and lipids in the sample ([*W*] and [*L*]) are obtained in Equation S2.

$$K \cong \frac{n_m}{n_a} \cdot \frac{[W]}{[L]} \quad \text{S3}$$

Since the concentration of peptide and lipids can usually be neglected with respect to the water concentration, [*W*] is essentially given by the number of moles of H_2O in a liter of pure water (approximately 55.5 M), and therefore it is a constant value. An apparent constant, with dimensions of molar concentration, can thus be defined as

$$K_{app.} = \frac{[W]}{K} \quad \text{S4}$$

In this way, equation S3 becomes

$$K_{app.} = \frac{n_a}{n_m} \cdot [L] \quad \text{S5}$$

Finally, it is possible to take into account the fact that each cell contains on average a given number of lipids. Therefore,

$$[L] \propto [cells] \quad \text{S6}$$

and it is possible to define a new apparent constant, with dimensions of cells/mL:

$$K_{app.}^{cells} = \frac{n_a}{n_m} \cdot [cells] \quad \text{S7}$$

The fraction of membrane-bound peptides is defined as

$$f_{bound} = \frac{n_m}{n_a + n_m} = \frac{n_m/n_a}{1 + n_m/n_a} \quad \text{S8}$$

Using Equation S7, this fraction can be expressed as:

$$f_{bound} = \frac{[cells]/K_{app.}^{cells}}{1 + [cells]/K_{app.}^{cells}} \quad \text{S9}$$

Equation S9 corresponds to Equation 1 in the main article, in the case of bacteria. It indicates a hyperbolic behavior of the fraction of membrane-bound peptides with the total cell density, and it does not depend on the total peptide concentration.

Supporting Figure 1 reports the experimental peptide/cell association curves (11). Equation 1 describes only approximately the experimental peptide/cell association data, which were also somewhat different for measurements performed with 1 or 10 μM peptide. This finding is not surprising, as the model is extremely simplified (for instance it does not treat explicitly electrostatic interactions, and it assumes that the number of bound peptides is always negligible with respect to the number of cell membrane lipids). However, Equation 1 can be considered as a useful first approximation if one is interested in describing the main features of the binding curves.

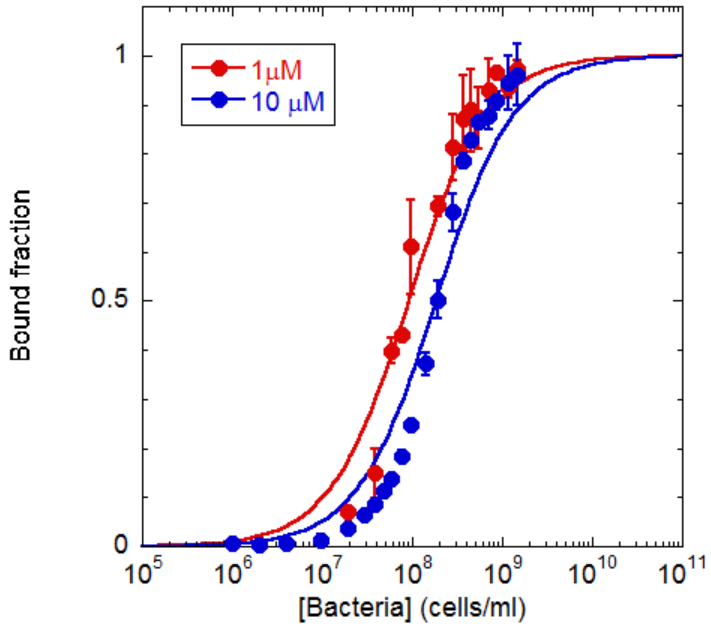

Supporting Figure 1 Fitting of the data for the association of DNS-PMAP23 to *E. coli* cells, at a peptide concentration of 1 or 10 μM (11) with Equation S9 (equivalent to Equation 1 in the main text).

Prediction of the minimum active (bactericidal or hemolytic) concentration.

In our previous study (11) we determined the threshold T_B of DNS-PMAP23 molecules that must bind to a single bacterial cell to cause its death. With this value, and the partition constant, it is possible to predict the minimum bactericidal concentration (MBC) at all values of cell densities. A similar treatment is possible for the hemolytic concentration in the case of erythrocytes. Therefore, in the following we will refer generally to a minimum active concentration.

The total number of membrane-bound peptide molecules can be expressed as

$$f_{bound}[P] \cdot V \cdot N_A \qquad \text{S10}$$

where $[P]$ is the total peptide molar concentration, N_A is Avogadro's constant and V is the sample volume (in liters).

The total number of cells in the sample is given by

$$[cells] \cdot V \cdot 10^3 \qquad \text{S11}$$

where [*cells*] is expressed in cells/mL, and 10^3 is the conversion factor between milliliters and liters. Combining these two equations, the average number of peptide molecules bound to each cell (N) can be calculated as

$$N = \frac{N_A}{10^3}\frac{f_{bound}}{[cells]}[P] \quad \text{S12}$$

The minimum active concentration (MAC, i.e. the MBC for bacteria and the MHC or the $HC_{50\%}$ for erythrocytes) corresponds to the peptide concentration for which N reaches the threshold value *T*, *i.e.*

$$T = \frac{N_A}{10^3}\frac{f_{bound}}{[cells]}MAC \quad \text{S13}$$

Inverting Equation S13, an expression for predicting the MAC is obtained

$$MAC = \frac{[cells]}{f_{bound}}\frac{10^3}{N_A}T \quad \text{S14}$$

Finally, if Equation S9 is substituted to the bound fraction, Equation S14 becomes

$$MAC = \left(1 + [cells]/K_{app.}^{cells}\right)\frac{10^3}{N_A}TK_{app.}^{cells} \quad \text{S15}$$

which corresponds to Equation 2 in the main text (in the case of bacteria).

Activity and toxicity in the presence of both bacterial and eukaryotic cells.

The goal of this section is to analyze the possible effects of the concomitant presence of two cell types (e.g. bacteria and erythrocytes), based on the partition equilibria described above. In this case, it is possible that both the MBC and the MHC increase (with respect to the values in the absence of the other cell type) because the two cell populations compete for peptide binding. The following equations will estimate how mixing the two cell populations reduces the amount of bound peptide to each cell type (under the same conditions of cell densities and peptide concentration).

In the presence of one cell type only, the fraction of peptide bound to bacteria or erythrocytes is defined by Equation S9:

$$f_B = \frac{[Bacteria]/K_{app.}^{B}}{1+[Bacteria]/K_{app.}^{B}} \quad \text{S16}$$

$$f_E = \frac{[Erythrocytes]/K_{app.}^{E}}{1+[Erythrocytes]/K_{app.}^{E}} \quad \text{S17}$$

By contrast, in the presence of both cell types, both partition equilibria must hold at the same time. From Equation S7 one obtains:

$$K_{app.}^{B} \cong \frac{n_a}{n_B} \cdot [Bacteria] \quad \text{S18}$$

$$K_{app.}^{E} \cong \frac{n_a}{n_E} \cdot [Erythrocytes] \quad \text{S19}$$

where n_B and n_E are the moles of peptide bound to the membranes of bacteria and to erythrocytes, respectively. In this case, the fraction of peptide bound to each cell type is defined as

$$f_B{}' = \frac{n_B}{n_a+n_B+n_E} \quad \text{S20}$$

$$f_E{}' = \frac{n_E}{n_a+n_B+n_E} \quad \text{S21}$$

Using the partition constants (Equations S18–S19), Equations S20–S21 become:

$$f_B{}' = \frac{[Bacteria]/K_{app.}^{B}}{1+[Bacteria]/K_{app.}^{B}+[Erythrocytes]/K_{app.}^{E}} \quad \text{S22}$$

$$f_E{}' = \frac{[Erythrocytes]/K_{app.}^{E}}{1+[Bacteria]/K_{app.}^{B}+[Erythrocytes]/K_{app.}^{E}} \quad \text{S23}$$

By comparing Equations S16–S17 and S22–S23, the ratios of the bound fractions in the absence and in the presence of the other cell population are obtained

$$\frac{f_B}{f_B'} = 1 + \frac{\frac{[Erythrocytes]}{K_{app.}^{E}}}{1+\frac{[Bacteria]}{K_{app.}^{B}}} \quad \text{S24}$$

$$\frac{f_E}{f_E'} = 1 + \frac{\frac{[Bacteria]}{K_{app.}^{B}}}{1+\frac{[Erythrocytes]}{K_{app.}^{E}}} \quad \text{S25}$$

These ratios are ≥1 and represent the predicted increase in MBC or MHC due to the concomitant presence of the other cell population. In the case of DNS-PMAP23, $K_{app.}^{B}$ = 1.8 x 10^8 cells/mL, $K_{app.}^{E} \sim 10^7$ cells/mL (see main text) and in experiments where both bacteria and RBCs were present we used [RBCs] = 4.5x10^8 cells/mL, [bacteria] = 4.5 x 10^7 cells/mL. Inserting these data in equations S24 and S25 one obtains $\frac{f_B}{f_B'} \sim 40$ and $\frac{f_E}{f_E'} \sim 1$. Therefore, based on the equilibrium model introduced above, one would expect a dramatic

reduction of the peptide molecules bound to bacteria, due to peptide sequestration by RBCs. This, in turn, should cause a drastic inhibition of the antibacterial peptide activity. By contrast, no significant inhibition is expected for the hemolytic activity. It is important to note that this conclusion is not dependent on the details of the equilibrium model, but simply on the prediction that a significant fraction of the peptide is bound to erythrocytes. Although $K_{app.}^{E}$ was estimated rather indirectly (Figure 2), its order of magnitude (10^7 cells/mL) should be correct, and therefore in the presence of 4.5 x 10^8 cells/mL most of the peptide should be bound to erythrocytes. Experimental data agree quite well with the simple equilibrium treatment described above when only one cell type is present (see Figure 1 in the main text). However, experiments were in contradiction with the model predictions when both host and target cells were present at the same time. This finding indicates that in the latter case other phenomena (e.g. the kinetics of peptide binding to the two cell types) are at play.

METHODS

Materials

The DNS-PMAP23 analogue (Dansyl-RIIDLLWRVRRPQKPKFVTVWV-NH_2), labeled with 5-(dimethylamino)naphthalene-1-sulfonyl (dansyl) at the N-terminus and amidated at the C-terminus, was purchased from AnyGen Co., while Esc(1–21) (GIFSKLAGKKIKNLLISGLKG-NH_2) was obtained from Chematek. In both cases, analytical RP-HPLC indicated a purity >98%and the molecular mass was verified by using MALDI-TOF. Bacterial culture media were purchased from Oxoid, and 96-well plates were from Falcon.

Antibacterial activity assay

Escherichia coli ATCC 25922 was grown in Luria-Bertani (LB) medium at 37 °C until a mid-log phase. Afterward, bacterial cells were centrifuged (1,400 x g for 10 min) and washed three times in buffer A (5 mM

HEPES, 110 mM KCl, 15 mM glucose, pH 7.3). Different concentrations of bacterial cells (as indicated in the results section) suspended in buffer A were added to different concentrations of DNS-PMAP23 (final volume of 100 µl) or to an equal volume of water for the negative control. Samples were then incubated at 37 °C and 800 rpm in a thermomixer (Eppendorf). After 120 min, aliquots of 5 µl were withdrawn, diluted in buffer A, and spread onto LB-agar plates. After overnight incubation at 37 °C, the number of CFUs was counted (29). Survival of bacterial cells was determined with respect to the negative control (see above). Bactericidal activity was defined as the peptide concentration necessary to cause a 10^3 times reduction in the number of CFUs, and determined by data interpolation. Data are the mean of three independent experiments ± standard deviation. The conditions used in this protocol (incubation in buffer A, 120 minutes incubation, a 10^3 times reduction in the number of CFUs for the definition of the MBC) were dictated by the necessity of comparing theoretical predictions and experimental data. Therefore, we used the same protocol employed in (11) to determine the minimum number of cell-membrane bound molecules needed to kill a bacterium and the partition data. In that study, we identified buffer A as a minimal culture medium where bacteria remain vital but do not multiply, maintaining a constant number of live cells for the 2 hours of incubation. Since no growth takes place under these conditions, we determined peptide activity by bacterial killing (MBC) rather than by the more common growth inhibition assays (MIC).

MIC was also determined, using a standard broth microdilution assay. Aliquots of 50 µl of bacteria in mid-log phase at a concentration of $2x10^5$ CFUs/mL in Mueller-Hinton (MH) broth were added to 50 µl of water containing the peptide in serial 2-fold dilutions. Antimicrobial activity was expressed as the minimal peptide concentration necessary to obtain 100% inhibition of microbial growth after 16–18 h of incubation at 37 °C.

Hemolytic activity assay

The hemolytic activity was measured on human red blood cells (RBCs), according to Mangoni *et al.* [(2011) *J. Med. Chem. 54,* 1298−1307]. Blood samples were obtained from healthy volunteers. Blood was washed

six times with 0.9% (w/v) NaCl, 5mM HEPES, pH 7.3, and resuspended in the same buffer. After this step, erythrocyte density was measured with an automated hematology analyzer Sysmex XE-2100 (Sysmex). Aliquots of the erythrocytes suspension, at a final concentration in the sample ranging from 4.5 x 10^8 to 4.5 x 10^5 RBCs/mL were incubated with serial two-fold dilutions of the peptide for 120 min at 37 °C with gentle mixing at 500 rpm in the thermomixer. The samples were then centrifuged and the absorbance of the supernatant was measured with different approaches, depending on the cell-density. For 4.5 x 10^8 and 4.5 x 10^7 RBCs/mL absorbance was measured at 540 nm using a sterile 96-well plate and a microplate reader (Infinite M200; Tecan). In the case of 4.5 x 10^8 RBCs/mL cell-density samples were diluted 3–10 times when absorbance of the undiluted samples was above 1.5. For 4.5 x 10^6 and 4.5 x 10^5 RBCs/mL absorbance was measured on a Jasco V-770 spectrophotometer (Jasco) at 414 nm (*i.e.* the wavelength of maximum absorbance of the Soret band) using 1 cm pathlength cuvettes. For the 4.5 x 10^6 RBCs/mL samples both methods (microplate reader and spectrophotometer) gave comparable results. The results are expressed as percentage hemolysis, calculated as follows: % hemolysis = $[(Abs_{sample} - Abs_{blank})/(Abs_{total\ lysis} - Abs_{blank})] \times 100$, where blank and total lysis consisted of erythrocytes suspended in physiological buffer and distilled water, respectively. $HC_{50\%}$ values were determined by data interpolation. Data are the mean of three independent experiments ± standard deviation.

Hemolytic and bactericidal activity assays in the presence of both RBCs and bacteria

The combination of 4.5 x10^8 RBCs/mL and 4.5 x 10^7 CFUs/mL of *E. coli* ATCC 25922 suspended in buffer A was used (final volume 110 µl). Control experiments demonstrated that under these conditions bacteria remain vital but do not multiply, maintaining a constant number of live cells for more than 15 minutes. At the same time, no significant spontaneous hemolysis was observed. Therefore, in order to have a stable and well defined number of cells in the sample for the whole duration of the experiment, in this assay cells were incubated with the peptide for 15 minutes only, by contrast to the MBC and hemolysis experiments of Figures 1 and 2. Fortunately, control experiments (Supporting Figure 2) showed that bacterial killing and hemolysis by DNS-PMAP23 are very fast, being essentially completed in the 15 minutes time-frame. Indeed,

data in Figures 1, 2 and 3 for the same cell densities are comparable. The activity of Esc(1–21) has been demonstrated to be completed within 15 minutes, too (29).

Samples were treated with DNS-PMAP23 at different concentrations, and incubated at 37 °C and 500 rpm in the thermomixer. After 15 min, 5 µl were withdrawn, diluted in water, and spread onto LB-agar plates for CFU counting after overnight incubation at 37 °C. The remaining volume was centrifuged and the absorbance of the supernatant was measured at 540 nm using a sterile 96-well plate, as described above. For comparison, experiments were performed also with RBCs or *E. co*li cells only, under the same conditions. Data are the mean of three independent experiments ± standard deviation.

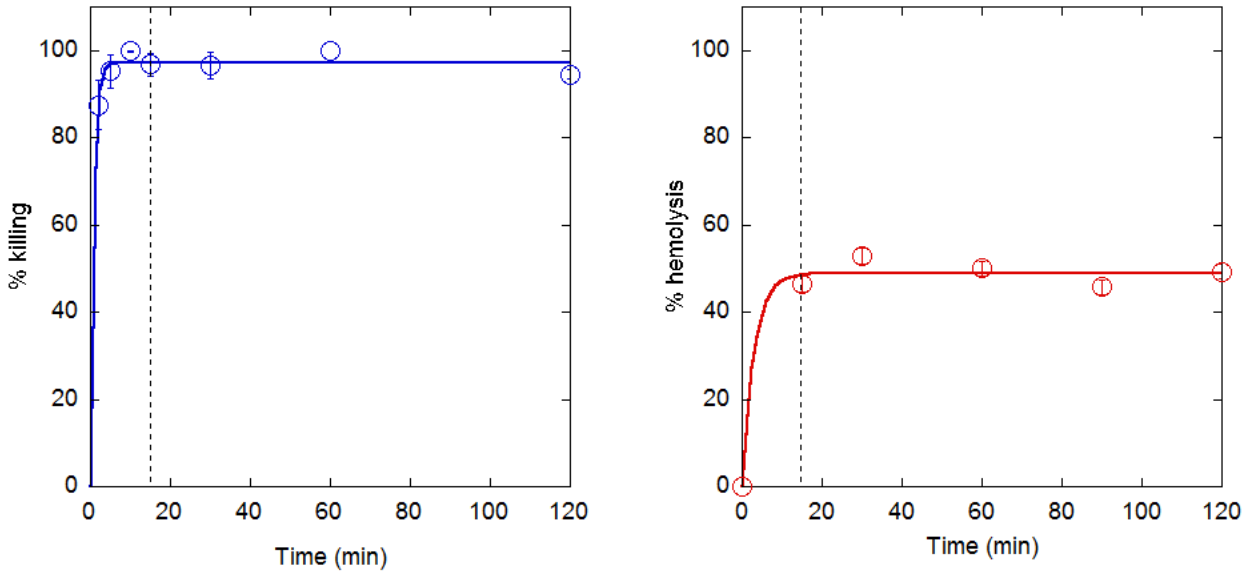

Supporting Figure 2. Kinetics of bacterial killing (left, 4.5 x 10^8 cells/mL) and hemolysis (right, 4.5 x 10^7 cells/mL) caused by 10 µM DNS-PMAP23. 15 minutes are indicated by a vertical dashed line.